Optical-model potential in nuclear matter from Reid's hard core interaction

J.-P. Jeukenne, A. Lejeune, and C. Mahaux
Theoretical Physics, University of Liège at Sart Tilman, B-4000-Liège I, Belgium
(Received 29 May 1974)

We describe a method for the calculation of the leading term of a previously proposed low-density expansion for the self-energy of nucleons in nuclear matter. We compute the single-particle complex potential energy, the average binding energy per nucleon, the complex symmetry potential, and the symmetry energy. We use Reid's hard core nucleon-nucleon interaction and take a Fermi momentum $k_F = 1.4$ fm^{-1}. The calculated single-particle potential energy is compared with the phenomenological values of the optical-model potential in the inner region of a nucleus. The real part of our theoretical value is given by $56 - 0.3E$ (MeV) below $E = 150$ MeV, and changes sign at 200 MeV. The imaginary part rises from 2 MeV at low energy to about 20 MeV at $E = 200$ MeV. These features are in good agreement with experimental evidence. The average binding energy B per nucleon calculated with a self-consistent potential energy for the particle states above k_F is equal to -11 MeV. In the standard approach, with no potential energy for intermediate particle states above k_F, one finds -8.65 MeV. We also calculate the symmetry potential. At low energy, its real part is equal to 14 $(N - Z)/A$ (MeV); it changes sign at 110 MeV. Its imaginary part is equal to 3.5 $(N - Z)/A$ (MeV) at low energy, and rises to 8.5 $(N - Z)/A$ (MeV) at 200 MeV. The symmetry energy is equal to 27.8 MeV.

[NUCLEAR REACTIONS Calculated complex optical-model potential, symmetry potential, average binding energy and symmetry energy for nucleons in nuclear matter, for a Fermi momentum equal to 1.4 fm^{-1}, from Reid's hard core nucleon-nucleon interaction, in the frame of Brueckner's theory]

I. INTRODUCTION

One of the original aims of Brueckner's theory[1,2] of nuclear matter was to reconcile the success of the shell-model with the strength and complexity of the nucleon-nucleon interaction. This implies not only the calculation of the average nuclear field, but also an evaluation of the mean free path of a nucleon inside the nucleus. At positive energy, this amounts to the calculation of the complex optical-model potential (OMP) from the nucleon-nucleon interaction. Most attempts in that direction have been limited either to the low[3-5] or to the high[6,7] energy regions, or used some simplified (usually separable) form for the nucleon-nucleon potential.[8-10] Recently, however, Kidwai and Rook[11] performed a calculation of the real part of the OMP in nuclear matter, starting from the Hamada-Johnston[12] nucleon-nucleon potential. Besides, several calculations were performed for the real[13-16] or imaginary[17-24] parts of the OMP in finite nuclei, usually starting from an effective nucleon-nucleon interaction. Some of these works include features typical of finite nuclei, like collective effects. However, they are usually limited to the low energy region, and often include only part of the absorption. Moreover, they lead to rather complicated, nonlocal, energy dependent OMP; these cannot be directly compared to the phenomenological ones, which contain no essential dependence on specific nuclear properties. Therefore, an approach based on the study of nuclear matter and on a realistic nucleon-nucleon interaction is of interest and is complementary to the calculations pertaining to particular nuclei. This is the point of view adopted in Refs. 3–5, 8–11, and in the present paper.

In nuclear matter, the concepts of target and of projectile lose their meaning. However, one can define a potential energy and a lifetime for a quasiparticle state, i.e., for the state obtained by creating a particle (or a hole) with momentum k on top of the correlated ground state. This can most conveniently be achieved in the frame of Green's function theory.[25] There, a mass (or self-energy) operator $M(\vec{r}, \vec{r}'; E)$ is introduced. In a translationally invariant and isotropic medium like nuclear matter, M is a function of only two variables, namely of $|\vec{r} - \vec{r}'|$ and E or, by Fourier transformation, of a momentum k and an energy E. It has been shown by Bell and Squires[26] that $M(\vec{r}, \vec{r}'; E)$ can be identified with the OMP, possibly after taking a suitable energy average.[27] Likewise, the potential energy and lifetime of a quasiparticle state in nuclear matter can be obtained from $M(k, E)$, and related to the real and imaginary parts of the OMP.[9,28] The present paper is concerned with a calculation of the leading

term of a low density expansion which has recently been proposed for $M(k, E)$.[29]

We establish our notation and describe our numerical procedure in Sec. II. In Sec. III, we present some numerical results obtained in the case of Reid's hard core nucleon-nucleon interaction[30] for $k_F = 1.4$ fm^{-1}. In Secs. III A and III B, we discuss the variation with energy of the real and imaginary parts, respectively, of the OMP in the inner region of a nucleus and we compare our results with the phenomenological values. In Sec. III C, we study the dependence with energy of the complex symmetry potential, in lowest order in the density. Section III D is devoted to the average binding energy per nucleon and to the symmetry energy. Section IV contains a brief discussion.

II. BASIC EQUATIONS AND COMPUTATIONAL PROCEDURE

We first briefly recall, in Sec. II A, the expression derived in Ref. 29 for the leading term of the low-density expansion of the mass operator, the corresponding expressions for the OMP, and the average binding energy per nucleon. Then, we describe our computational procedure in Secs. II B and II C.

A. Basic equations

The single-particle Green function $G(k, E)$ is related to the mass operator $M(k, E)$ by[25] ($\hbar = 1$)

$$G(k, E) = [E - k^2/2m - M(k, E)]^{-1} , \tag{1}$$

where m is the nucleon mass. It has poles at the roots of the equation

$$\omega_k = k^2/2m + M(k, \omega_k) . \tag{2}$$

The real part of ω_k gives the energy of a quasiparticle with momentum k. Its imaginary part is equal to half the spreading width of a single-particle state and can be identified with the imaginary part of the OMP.[9,28] Let us expand ω_k about the real quantity

$$\epsilon_k = k^2/2m + \mathrm{Re}\, M(k, \epsilon_k) = k^2/2m - V_k . \tag{3}$$

The symbols Re and Im stand for the "real part of" and "imaginary part of," respectively. Keeping only the first order term, we find

$$G(k, E) \simeq \frac{\rho_k}{E - \bar{\epsilon}_k + i\bar{W}_k} , \tag{4}$$

where

$$\bar{\epsilon}_k - i\bar{W}_k = \epsilon_k + i\rho_k \,\mathrm{Im}\, M(k, \epsilon_k) , \tag{5}$$

$$\rho_k = \left[1 - \frac{\partial M(k, E)}{\partial E}\right]^{-1}_{E=\epsilon_k} . \tag{6}$$

In nuclear matter, one has[9]

$$a_k = F_k \left[\frac{\partial \,\mathrm{Im}\, M(k, E)}{\partial E}\right]_{E=\epsilon_k} \ll 1 , \tag{7}$$

where

$$F_k = \left[1 - \frac{\partial \,\mathrm{Re}\, M(k, E)}{\partial E}\right]^{-1}_{E=\epsilon_k} . \tag{8}$$

Thus, we can write

$$\bar{\epsilon}_k \simeq \epsilon_k + a_k \bar{W}_k , \quad \bar{W}_k \simeq F_k W_k , \tag{9}$$

with

$$W_k = -\,\mathrm{Im}\, M(k, \epsilon_k) . \tag{10}$$

Equations (3), (7) and (4) show that the real part of the OMP can be identified with

$$-\bar{V}_k = \mathrm{Re}\, M(k, \epsilon_k) + a_k \bar{W}_k = -V_k + a_k \bar{W}_k , \tag{11}$$

and its imaginary part with W_k. In lowest order in the density, $F_k \simeq 1$.[29] This, together with inequality (7), gives

$$\mathrm{Re\,OMP} \simeq -V_k , \quad \mathrm{Im\,OMP} \simeq -W_k . \tag{12}$$

Since the differences between V_k and $\bar{V}_k$ and between W_k and $\bar{W}_k$ are of second order in the density,[29] approximations (12) are consistent with the fact that we calculate only the leading term of the low-density expansion of $M(k, E)$. We now turn to the description of this leading term.

We introduce the notation[29]

$$\begin{aligned} n_>(a) = 1 - n_<(a) = 0 \quad &\text{if } a < k_F , \\ = 1 \quad &\text{if } a > k_F . \end{aligned} \tag{13}$$

We denote by v the nucleon-nucleon potential, and by $|\vec{a}, \vec{b}\rangle$ the product of two plane waves with momenta $\vec{a}$ and $\vec{b}$, respectively. We define a complex reaction matrix by the integral equation

$$g(w) = v + \sum_{\vec{a},\vec{b}} n_>(a) n_>(b) v \frac{|\vec{a}, \vec{b}\rangle\langle\vec{a}, \vec{b}|}{w - e(a) - e(b) + i\delta} g(w) , \tag{14}$$

where

$$e(a) = a^2/2m + U(a) . \tag{15}$$

Here, $U(a)$ is an auxiliary potential which should be chosen such as to optimize the convergence of the low density expansion for the mass operator, whose leading term reads[29]

$$M_I(k, E) = \sum_{\vec{j}} n_<(j) \langle \vec{k}, \vec{j}\,| g(E + e(j)) |\vec{k}, \vec{j}\rangle_A . \tag{16}$$

Here, the index A refers to antisymmetrization. It is argued in Ref. 29 that $U(d)$ should be taken self-consistently

$$U(d) = \mathrm{Re}\, M(d, \bar{\epsilon}_d) , \tag{17}$$

which in lowest order reduces to

$$U(d)=\mathrm{Re}\,M_I(d,\epsilon_d)\ . \tag{18}$$

The average binding energy per nucleon B can, in lowest order, be calculated from the relation

$$B=\frac{3}{5}\frac{k_F^2}{2m}+\frac{1}{2}\sum_{\vec{j},\vec{k}} n_<(j)n_<(k)\langle\vec{k},\vec{j}|g(e(k)+e(j))|\vec{k},\vec{j}\rangle_A\ . \tag{19}$$

Relations (16) and (18) imply that $U(d)$ is continuous at $d=k_F$. In the recent calculations of the average binding energy per nucleon, one uses Eq. (19) with, however, an auxiliary potential $U(a)$ equal to zero in particle states ($a>k_F$), and taken self-consistently for hole states ($a<k_F$). In these calculations, the auxiliary potential thus displays a gap at k_F.[2,31] Auxiliary potentials without gap (or with a very small one to avoid singularities) have been used in different but related contexts.[32-39]

B. Method of solution

Equation (14) is formally identical to the familiar Bethe-Goldstone equation encountered in binding energy calculations.[1,2] Its solution involves, however, three additional difficulties. (i) The operator g is non-Hermitian. (ii) The kernel is singular for $w=e(a)+e(b)-i\delta$. (iii) The self-consistent condition (18) must be fulfilled for $d>k_F$ as well as for $d<k_F$. None of these difficulties is by itself a critical one, but their simultaneous existence required a careful search for a computational procedure which combines accuracy and sufficient rapidity. Difficulties (i) and (ii) reflect the fact that the defect function[2] [Eq. (33) below] does not vanish at large distance (no healing), so that the convenient reference spectrum method[2] presumably cannot be used as a starting point. In particular, the procedure of Ref. 11 is questionable.[40] Here, we transform Eq. (14) into a set of linear equations by discretizing the kernel. Two main methods exist, based on a coordinate space[1] and on a momentum space[41] representation, respectively. We adopt here the former one. We follow closely the procedure of Brueckner and Gammel[1] and introduce the quantities

$$\vec{p}=\vec{a}+\vec{b},\quad \vec{t}=\tfrac{1}{2}(\vec{a}-\vec{b})\ , \tag{20}$$

$$\vec{p}_+=\tfrac{1}{2}\vec{p}+\vec{t},\quad \vec{p}_-=\tfrac{1}{2}\vec{p}-\vec{t}\ , \tag{21}$$

$$f(p,t)=1 \quad \text{if } p_+ \text{ and } p_->k\ ,$$
$$=0 \quad \text{otherwise}\ . \tag{22}$$

Henceforth, we consider the case of a potential v with a hard core of radius r_c which we shall treat like a hollow core.[1] The correlated two-nucleon wave function $\psi_w(\vec{k},\vec{j})$ is defined by

$$v\psi_w(\vec{k},\vec{j})=g(w)|\vec{k},\vec{j}\rangle\ . \tag{23}$$

It can be expanded into partial waves, provided the quantities $f(p,t)$ and $e(a)+e(b)$ are replaced by their angle averages, namely[1,42]

$$p_\pm=\tfrac{1}{4}p^2+t^2\pm 3^{-1/2}f(p,t)pt\ ; \tag{24}$$

if $\frac{1}{2}p<k_F$,

$$f(p,t)=0 \quad \text{if } (t^2+\tfrac{1}{4}p^2)^{1/2}<k_F$$
$$=1 \quad \text{if } t-\tfrac{1}{2}p>k_F \tag{25}$$
$$=\frac{t^2+\frac{1}{4}p^2-k_F^2}{tp} \text{ otherwise}\ ;$$

if $\frac{1}{2}p>k_F$,

$$f(p,t)=1 \quad \text{if } |t-\tfrac{1}{2}p|>k_F$$
$$=\frac{t^2+\frac{1}{4}p^2-k_F^2}{tp} \text{ otherwise.} \tag{26}$$

We introduce the quantities

$$B_l(r,r',t)=\frac{1}{2\pi^2}j_l(tr)j_l(tr')f_l(p,t)\ , \tag{27}$$

$$G_l(r,r';w)=P\int_0^\infty t^2\frac{B_l(r,r',t)}{w-e(p_+)-e(p_-)}\,dt$$
$$+i\pi t_0^2 B_l(r,r',t_0)$$
$$\times\left\{\frac{d}{dt}[e(p_+)+e(p_-)]\right\}^{-1}_{t=t_0}\ . \tag{28}$$

Here, P denotes a principal value integral, while t_0 is the real root of the equation

$$w-e(p_+)-e(p_-)=0\ . \tag{29}$$

We denote by J, S, l and l' the two-nucleon total angular momentum, total spin, initial and final orbital angular momenta, respectively. The radial parts of $\psi_w(\vec{k},\vec{j})$ are given by the integral equations

$$u^{JS}_{ll',w}(qr)=s_{l,w}(qr)\delta_{ll'}+4\pi\sum_{l''}\int_{r_c}^\infty r'^2\,F_{l'}(r,r';w)v^{JS}_{l'l''}(r')u^{JS}_{ll'',w}(qr')dr'\ , \tag{30}$$

where $v^{JS}_{l'l''}$ is the standard potential matrix, while

$$\vec{q}=\tfrac{1}{2}(\vec{k}-\vec{j}) ,$$

$$s_{l,w}(qr)=j_l(qr)-j_l(qr_c)\frac{G_l(r,r_c;w)}{G_l(r_c,r_c;w)} , \tag{31}$$

$$F_l(r,r';w)=G_l(r,r';w)-\frac{G_l(r,r_c;w)G_l(r_c,r';w)}{G_l(r_c,r_c;w)} . \tag{32}$$

The defect function

$$\chi^{JS}_{ll'w}(qr)=u^{JS}_{ll,w}(qr)-s_{l,w}(qr) \tag{33}$$

does not heal for $w>2\,e(k_F)$. The leading term of the low density expansion for the mass operator is found equal to

$$M_I(k,E)=\sum_{\vec{j}} n_<(\vec{j})\sum_{T=0}^{1}\sum_{S=0}^{1}\tfrac{1}{2}(2T+1)Q(S,T,\vec{j},q;e(j)+E) , \tag{34}$$

where T refers to the two-nucleon total isospin, and

$$Q(S,T,\vec{j},q;w)=4\pi\sum_J(2J+1)\sum_{l=J-1}^{J+1}\left[\frac{j_l^2(qr_c)}{4\pi G_l(r_c,r_c;w)}+\int_{r_c}^{\infty}r^2 s_{lw}(qr)\sum_{l'=J-1}^{J+1}v^{JS}_{ll'}(r)u^{JS}_{ll',w}(qr)dr\right] . \tag{35}$$

C. Computational procedure

We replace in Eq. (30) the integral by a sum of trapezoids with the mesh points $(r,r')=r_c$, 0.575, 0.6, 0.65, 0.7, 0.8, 0.9, (0.2), 1.7, (0.4), 2.9, 3.5, 4.5, and 5.4 fm, and obtain a set of complex linear equations. The same mesh points are used in the calculation of the integral in Eq. (35). The sum over $\vec{j}$ in Eq. (34) implies an integral over j and over the angle θ between $\vec{j}$ and $\vec{k}$. We checked that one can limit oneself to the two values $\cos\theta=\pm\sqrt{3}$, as proposed in Ref. 1. Likewise, the two values $j=0.58$ and 0.93 are sufficient for $k<0.9\,k_F$. However, caution must be exercised for $k>k_F$. For k close to k_F, the behavior[29] $W_k\propto(k^2-k_F^2)^2$ [Eq. (43) below] results from the fact that the imaginary part of Q in Eq. (34) vanishes unless j is close to k_F. This led us to calculate W_k by taking seven equally spaced values for j in the domain where ImQ does not vanish. We imposed the self-consistency condition (18) at eight values for k, namely $k/k_F=0.1$, 0.5, 0.9, 1.2, 1.6, 2.0, 2.4, and 3.0. We shall see in Sec. III that the omission of the imaginary part of $G_l(r,r';w)$ has only a small influence on $U(d)$. Therefore, this approximation was made in the search for self-consistency, except in the last two iterations.

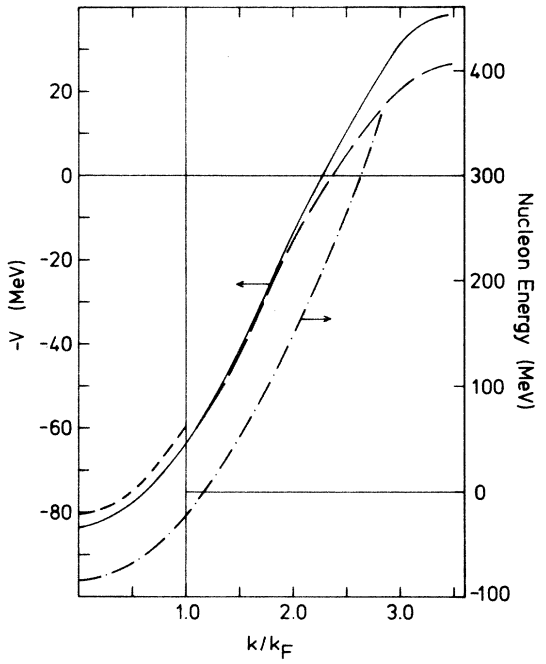

FIG. 1. The potential energy ($-V_k$) and the energy $E=\epsilon_k$ [Eq. (3)] are plotted versus k/k_F. The full curve gives ($-V_k$) when the imaginary part of G_l [Eq. (28)] is neglected; the long dashes include the effect of this imaginary part. The short dashes result from the choice $U=0$ [Eq. (15)] in the intermediate states. The dash and dots (right-hand scale) shows the energy E obtained by subtracting V_k from the kinetic energy.

As emphasized in Ref. 1, the most consuming part of the program is the calculation of the functions $G_l(r,r';w)$, which must be performed many times. The contribution from the values $t>t_M=10$ fm^{-1} to the integral in Eq. (28) was obtained from the asymptotic formula (91) of Ref. 1. The remainder of the principal value integral is written in the form

$$P\int_0^{t_M}\frac{t^2A_l(r,r',t)-t_0^2A_l(r,r',t_0)}{t^2-t_0^2}\,dt - \tfrac{1}{2}t_0A_l(r,r',t_0)\ln\frac{t_M+t_0}{t_M-t_0} , \tag{36}$$

where

$$A_l(r,r',t)=\frac{(t^2-t_0^2)B_l(r,r',t)}{w-e(p_+)-e(p_-)} . \tag{37}$$

We compute the denominator in Eq. (37) from analytical expressions fitted to the calculated values $U(d)$ by the least squares method. We use two polynomials of the form $A+Bk^2+Ck^4$ in the domains $k<1.2k_F$ and $k_F<k<2.0k_F$, respectively, and a Woods-Saxon form in the region $1.8k_F<k$. These regions overlap, so that the over-all function is smooth. The Woods-Saxon shape was adopted because we observed that $U(d)$ approaches a constant for large values of d. The quantity $A_l(r, r', t_0)$ used in Eq. (36) may be obtained by interpolating Eq. (37). The integral in Eq. (36) is evaluated by Simpson's three point rule, using 41 points in the domain $0<t<4$ fm^{-1} and 11 points in the region 4 fm$^{-1}<t<t_M$. We also check and exploit the fact that $G_l(r, r'; w)$ can be interpolated over r' and w.

The accuracy of the final program was tested in two ways. Firstly, we set $U(d)=0$ and $f(p, t)=1$. Then the calculated reaction-matrix should reduce to the free nucleon-nucleon transition matrix. Secondly, we made the standard choice $U(a)=0$ for $a>k_F$, and compared our calculated contributions of the different partial waves to the average binding energy with those obtained by Siemens[43] from a different method.[44] These two checks indicate that our accuracy is better than 5%.

III. NUMERICAL RESULTS

In the present section, we discuss the numerical results which we obtained from Reid's hard core potential,[30] in the case $k_F=1.4$ fm^{-1}. We include the contributions from the S and D partial waves with $J\leq 2$ and from the P partial waves.

A. Real part of the OMP

The dependence of V_k [Eq. (11)] upon k/k_F is shown in Fig. 1. The full curve represents the value calculated when the imaginary part of G_l [Eq. (28)] is dropped, the long dashes include the influence of the imaginary part. As announced in Sec. II C, the difference between the two curves is small, except for $k/k_F>2.5$. The short dashes give the values obtained for V_k below k_F, when one sets $U(a)=0$ for particle states ($a>k_F$) as in standard binding energy calculations. The suppression of the gap thus increases the absolute magnitude of the potential energy of hole states. We return to this point in Sec. III D. We note that V_k changes sign at $k/k_F=2.4$, which implies a change of sign at the corresponding energy (200 MeV). For large values of k, V_k appears to approach a constant which is determined by the fit to be 45 MeV for the dashed curve. This asymptotic value is, however, not accurately determined, since no fully self-consistent calculation was performed beyond $k/k_F=3.0$. Locally, the dependence of V_k upon k can be fitted with a parabola, and an effective mass m^* can be defined by

$$m^*=m\left\{1+m\hbar^{-2}k^{-1}\frac{dV_k}{dk}\right\}^{-1}. \tag{38}$$

The ratio m^*/m corresponding to the full curve in Fig. 1 equals 0.68 at $k<k_F$, and 0.9 at $k=3k_F$, with an approximately linear increase between k_F and $3k_F$. The effective mass corresponding to the short dashes in Fig. 1, i.e., to the case of a vanishing potential energy in particle states, is equal to 0.63 m. It was noted previously[32,37,38] that the suppression of the gap at k_F increases the effective mass below k_F. This increase, however, is too small to bring the effective mass close to its phenomenological value[45] $m^*\simeq m$ in the vicinity of k_F. It appears that higher order corrections or collective effects play in important role for the effective mass at and below k_F.[35,37,38,46] The effective mass for $k>k_F$ is related to the energy dependence of the OMP. We shall see below that our results are in fair agreement with the phenomenological effective mass at positive energies.

Equation (3) determines the energy of a nucleon of momentum k. The dash and dots in Fig. 1 (right-hand scale) represent the momentum dependence of this energy E, calculated from the leading term M_I of the low density expansion, i.e., by subtracting V_k from the kinetic energy. We note that $E=0$ at $k=1.7k_F$ and that $E=-22.8$ MeV at $k=k_F$. The relation between the latter value and the average binding energy per nucleon is discussed in Sec. III D.

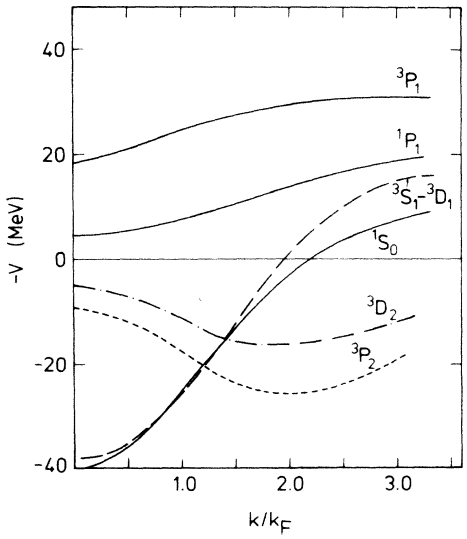

FIG. 2. Momentum dependence of the main partial wave contributions to the potential energy ($-V_k$).

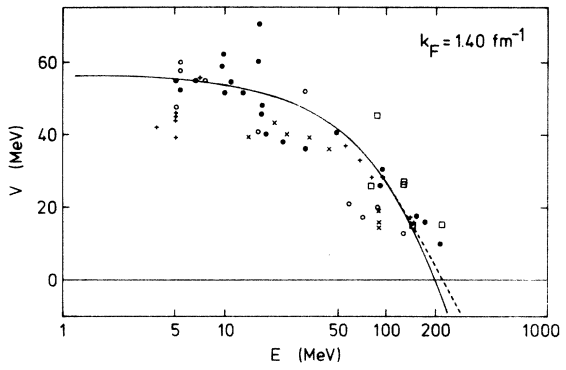

FIG. 3. The values for V_k calculated with (short dashes) and without (full curve) the imaginary part of G_l are compared with the phenomenological depths compiled by Passatore (Ref. 48). The origin of the data points is specified in Sec. III A.

The contributions of various partial waves to $-V_k$ are shown in Fig. 2. Below k_F, the S partial waves dominate, while the contributions of the P and D partial waves approximately cancel each other, as known from previous binding energy calculations.[2] When the energy increases, however, the contribution of the S partial waves and also the depth of the OMP decrease. The potential becomes repulsive at $E = 200$ MeV, in fair agreement with the careful analysis performed by Elton[47] of the interaction of 180 MeV protons with ^{56}Fe.

From the full and dash and dots curves in Fig. 1, we obtain the dependence of V_k upon energy which is shown in Fig. 3 (full curve). The dotted curve includes the effect of the imaginary part (long dashes in Fig. 1). The points in Fig. 3 represent the values compiled by Passatore[48] from previous phenomenological analyses. The + 's refer to neutron scattering with volume absorption, the ×'s to neutrons with surface absorption, the full dots to protons with volume absorption, the open dots to protons with surface absorption, and the squares to semiclassical analyses of proton scattering. We see that our theoretical curve reproduces the main trend of the phenomenological values which, however, show considerable scatter. A more consistent and a reliable set of phenomenological values is provided by Bowen *et al.*[49] and shown in Fig. 4. These authors make special use of the maxima and minima in the total neutron cross sections of the nuclei indicated on top of each point. The full curve is the same as that shown in Fig. 3, and corresponds to the linear law

$$V_k(E) = 56.5 - 0.3E \text{ (MeV)},$$

$$20 \text{ MeV} < E < 150 \text{ MeV} . \quad (39)$$

This theoretical law refers to nuclear matter with equal number of neutrons and protons. The dotted line in Fig. 4 shows the theoretical values obtained by subtracting from the full curve the symmetry potential obtained from Fig. 9 below.

The analysis of the scattering from a particular nucleus at different energies also provides a reliable way of studying the energy dependence of the real part of the OMP. Figure 5 shows the values obtained in Refs. 50 and 51, for the scattering of protons by ^{58}Ni (crosses) and ^{40}Ca (full dots), respectively, together with our theoretical values (full line).

Becchetti and Greenlees[52] give the phenomenological values ($N = Z$)

$$V_k = 54 - 0.32E, \quad (E < 50 \text{ MeV}) \quad (40)$$

for the depth of the real part of the OMP obtained

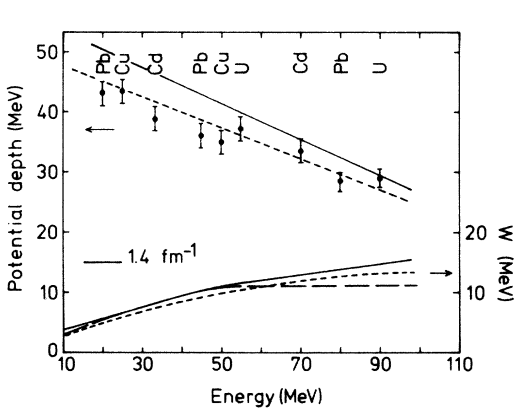

FIG. 4. The calculated values for V_k (left-hand scale, full curve in Fig. 1) and W_k (right-hand scale, full curve in Fig. 6) are compared with the experimental values of Ref. 49 for the real (full dots) and imaginary (long dashes) parts of the OMP, respectively. The short dashes are obtained by subtracting the symmetry potential (Fig. 9).

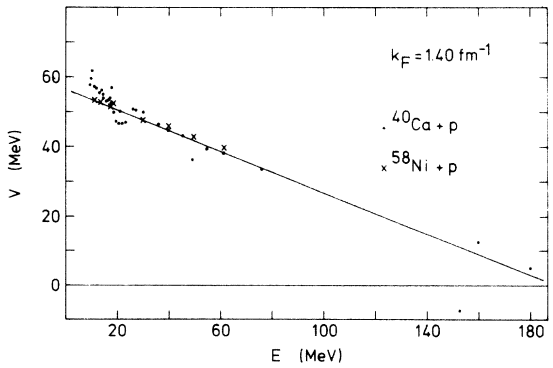

FIG. 5. Comparison between the calculated values for V_k and the values obtained from the scattering of protons from ^{40}Ca (full dots, Ref. 51) and ^{58}Ni (crosses, Ref. 50).

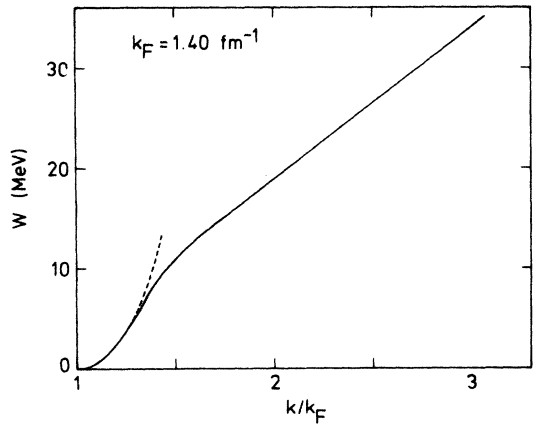

FIG. 6. Dependence of W_k [Eq. (10)] upon k/k_F (full curve). The dotted curve represents the asymptotic expression (43), with $N = 9.6$.

for the scattering of protons and

$$V_n = 56.3 - 0.32E, \quad (E < 50 \text{ MeV}) \tag{41}$$

in the case of neutrons. Both values are in good agreement with our results. The energy dependence quoted by Perey[53] for 9-MeV to 22-MeV protons is

$$V = 53.3 - 0.55E \ . \tag{42}$$

However, the coefficient of E is reduced to 0.3 when the influence of the first inelastic channel on the OMP is omitted. Our nuclear matter calculation does not include the effect of this transition to a low-lying *collective* state.[53] In other words, it yields the potential which would be included in a coupled channel calculation where this coupling is treated explicitly. Finally, we recall that the coefficient of E is rather accurately determined by the data, but that the constant (value at $E = 0$) is more sensitive to the geometry (radius, diffuseness) adopted for the fit.

B. Imaginary part of the OMP

The variation with k/k_F of the quantity W_k defined in Eq. (10) is shown in Fig. 6 (full curve). At low energy, the following asymptotic law holds[3,54]:

$$W_k = \frac{m^*}{4m^3}\left(\frac{k^2 - k_F^2}{N}\right)^2 . \tag{43}$$

The dotted curve in Fig. 6 represents Eq. (43), with $N = 9.6$ MeV. The latter value is in fair agreement with previous estimates by Brueckner, Eden, and Francis[3] ($N = 8.4$), Shaw[4] ($N = 10.5$ and 9.5), and Hüfner and Mahaux[29] ($N = 11.8$), for various interactions. We see that the asymptotic law (43) is justified only up to $k = 1.25k_F$, i.e., for $E < 10$ MeV (Fig. 1). Figure 7 shows the contribution to $-W_k$ of various partial waves. At low energy the S partial waves dominate, as expected. For $E > 50$ MeV, however, the higher partial waves play a significant role. This may be at the origin of the difference between our results and those of Reiner,[9] who only includes S waves (and also uses a different approach). The importance of the $^3P_1$ and $^1P_1$ partial waves above 150 MeV is particularly striking. This can be understood from the impulse approximation and the fact that the corresponding nucleon-nucleon phase shifts are large and steadily increasing in absolute magnitude. The variation of W_k with energy is shown in Fig. 8 (full curve), together with the phenomenological values compiled by Passatore.[48] The conventions are the same as in Fig. 3 with, in addition, full

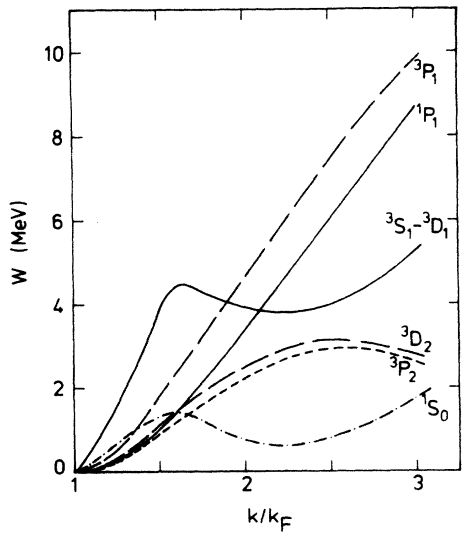

FIG. 7. Momentum dependence of the main partial wave contributions to the imaginary part W_k.

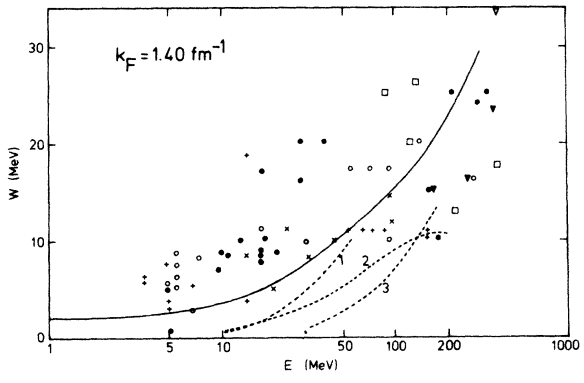

FIG. 8. Comparison between the calculated values of W_k (Fig. 7) and the phenomenological values compiled by Passatore (Ref. 48).

triangles for values obtained from the nucleon-nucleon total cross section and an open triangle from $p-{}^{12}C$ scattering. The scatter of the phenomenological values is even larger than in the case of the real part. This is related to their sensitivity to the type of analysis, for instance to the radial shape which is assumed. The curves marked 1, 2, and 3 in Fig. 8 refer to the value of W_k at the center of the nucleus used in Refs. 52, 55, and 56, respectively. Curve 3 is probably artificially lowered by the assumption[53] that the absorption is predominantly surface peaked up to about 120 MeV, while it appears to take a volume shape already at lower energies.[52] The phenomenological value for the depth of the volume absorption part appearing in Ref. 52 reads, for neutron (curve marked "1" in Fig. 8):

$$W_k = 0.22E - 1.56, \quad 10\ \text{MeV} < E < 50\ \text{MeV}, \tag{44}$$

to be compared with our theoretical result

$$W_k \simeq 0.19E + 1.9, \quad 10\ \text{MeV} < E < 60\ \text{MeV}. \tag{45}$$

The long dashes in Fig. 4 represent the phenomenological values of W_k obtained by Bowen *et al.*[49] from their detailed analysis, while the full curve represents our theoretical results, for equal number of protons and neutrons. The dotted curve is obtained by subtracting from the full curve the complex part of the symmetry potential calculated below in Sec. III C.

It has been shown by Perey and Buck[57] and by Wilmore and Hodgson[58] that the differential neutron elastic scattering cross sections below 25 MeV can be fitted with an OMP whose imaginary part is independent of energy and has only a surface component. This has been taken as an indication that the Fermi gas model is invalid,[54] since the latter predicts the low energy behavior (43). However, we recall that this asymptotic behavior is not valid above 10 MeV, where the calculated increase of W_k becomes smaller. Furthermore, the scattering data at low energy are not sensitive to the absorption in the inner region, and good fits can also be obtained with W_k's which increase with energy in the inner region.[53] Perey[59] mentions that the analysis of inelastic cross sections seems to imply an energy dependent W_k at low energy. Finally, we note that Elton[47] finds $W_k = 20$ MeV in a detailed analysis of the interaction of 180-MeV protons with ${}^{56}Fe$; we obtain $W_k = 21$ MeV at that energy.

C. Symmetry potential

The preceding calculations refer to nuclear matter with equal number of protons (Z) and of neutrons (N). In the present section, we calculate from Eq. (34) the difference between proton and neutron potential energies when slightly different Fermi momenta are taken for protons and neutrons. We neglect the dependence of Q [Eq. (35)] upon k_F, which gives only a small contribution.[5] Thus, we compute that part of the symmetry potential which arises from the occurrence of two different integration limits in the sum over j in Eq. (34), when $N \neq Z$. We write the difference between proton and neutron potentials in the form ($A = N + Z$):

$$(V_p - V_n) + i(W_p - W_n) = (V_T + iW_T)\frac{N-Z}{A}. \tag{46}$$

The expression of V_T and W_T can easily be obtained from Eq. (34), by following the same procedure as in Refs. 5 and 60:

$$V_T + iW_T = \frac{1}{12\pi^2} k_F{}^3 \int_0^{\pi} \sin\theta \sum_{T=0}^{1} (2T-1) \sum_{S=0}^{1} Q(S, T, \vec{k}_F, q; e(j) + e(k)) d\theta, \tag{47}$$

where θ refers to the angle between $\vec{k}_F$ and $\vec{k}$. For $k = k_F$, we find $V_T = 31$ MeV, in comparison with the values $V_T = 20$ MeV obtained by Brueckner and Dabrowski[60] and $V_T = 36$ MeV given by Azziz,[5] who used different potentials and Fermi momenta. The calculated variations of V_T and W_T with energy are shown in Fig. 9. At low energy, V_T equals about 25 MeV, while most phenomenological values range from 40 to 60 MeV.[61] This disagreement is generally attributed to the rearrangements effects[5,60] which are of higher order in the density and therefore fall outside the scope of the present paper. Their contribution at $k = k_F$ has been estimated in Refs. 5 and 60. However, no energy dependence appears to have been calculated yet. Our value for V_T changes sign at 110 MeV. Recently, some empirical evidence has been found for such a decrease of V_T with energy.[62] We note that the rearrangement contributions to the mass operator are real[29] and that they influence W_T only indirectly, via the self-consistent requirement. Unfortunately, very little is known about the phenomenological values of W_T, especially in the inner region of a nucleus.[61,62] Our results for V_T and W_T are

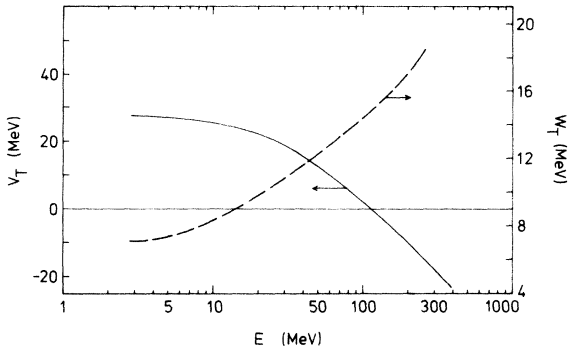

FIG. 9. Energy dependence of V_T (full curve, left-hand scale) and W_T (dashes, right-hand scale) [Eq. (47)]. These quantities are equal to $A/(N-Z)$ times the difference between the depths for protons and neutrons, and are therefore twice larger than the standard definition of the symmetry potentials.

similar to those obtained by Dabrowski and Sobiczewski,[63] who used the impulse approximation.

D. Binding energy and symmetry energy

The average binding energy per nucleon is given by Eq. (19). This expression is formally identical to the one appearing in standard calculations.[2] However, we use here a different self-consistent prescription for particle states ($k > k_F$). In particular, the auxiliary potential U presents no gap at k_F. From our calculation, we find $B = -11$ MeV at 1.4 fm^{-1}, while the value obtained with $U = 0$ for particle states equals −8.65 MeV. As expected,[2] the suppression of the gap at k_F increases the value of the two-hole line contribution [Eq. (19)]; the fact that U is repulsive above k_F also increases the binding. We recall that our prescription for U has been based on the consideration of the physical single-particle potential energy. Hence, it is not necessarily a favorable one for the binding energy. We also note that the Fermi energy $\epsilon_F = E(k_F)$ is equal to −22.8 MeV (Fig. 1). The exact value of the Fermi energy should be equal to the average binding energy per nucleon,[64] at the saturation density. The difference between our calculated values for ϵ_F and B can be attributed to the rearrangement potential[65] and to the fact that the saturation density may differ from 1.4 fm^{-1}. The rearrangement contributions decrease with energy[65,66] and presumably have only little effect on the optical potential at positive energies, except for the symmetry and spin-spin terms.[67] Finally, we compute the symmetry energy with the same approximation as for the symmetry potential in Sec. III C and find 27.8 MeV. The empirical value is close to 30 MeV.[2]

IV. DISCUSSION AND SUMMARY

We have studied the leading term of a low density expansion for the complex potential energy of a nucleon, in nuclear matter with Fermi momentum $k_F = 1.4$ fm^{-1}. We used Reid's hard core interaction and did not adjust any parameter in the course of the calculation. The real part of the calculated potential is given by (in MeV)

$$V_k = 56 - 0.3E \quad (10 \text{ MeV} < E < 180 \text{ MeV}). \tag{48}$$

The result is in good agreement with the phenomenological values. The potential depth had previously been calculated from different theoretical approaches and for various interactions. In Refs. 9 and 10, the authors used independent pair approximations derived from the Martin-Schwinger equations[68] connecting the one-, two-,... body Green functions. They take separable interactions and are led to expressions similar to Eqs. (14) and (16) with, however, different prescriptions for U and for the Pauli operator. Their calculated values for V_k are larger than the phenomenological ones. Equation (16) was also used by Kidwai and Rook[11] who, however, do not take fully self-consistent potential energies and calculated only the real part of the potential. They solve Eq. (14) by a modified version of the reference spectrum method.[2] They use the Hamada-Johnston nucleon-nucleon interaction[12] and find

$$V_k = 63 - 0.28E, \tag{49}$$

which is remarkably close to Eq. (48).

The imaginary part of the OMP at low energy was calculated by Shaw[4] on the basis of Eq. (16) without, however, a fully self-consistent requirement. His approximation is probably reliable at low energy. Using the matrix elements calculated in Ref. 1, he finds $W_k \simeq 0.3E$ (5 MeV $< E <$ 15 MeV). This is close to our result in this energy range. The imaginary part W_k was also calculated in Refs. 9 and 10. Reiner[9] finds a maximum ($W_k = 12.5$ MeV) at 200 MeV, which is probably related to his restriction to S waves, as mentioned in Sec. III C. Ho-Kim and Khanna[10] obtain $W_k = 2.4 + 0.009E$ (MeV) from an approximation similar to that used in Ref. 9, but a different nucleon-nucleon interaction. The imaginary part of the OMP at low energy has also been evaluated from the nucleon-nucleon cross sections.[69,70]

One may wonder whether the rather good agreement between our results and the phenomenological values will not be spoiled by the higher order terms in the density expression. The investigation of some of these corrections is in progress. Preliminary results indicate that they appear to de-

crease the values of V_k and W_k. They become fairly small at positive energies; this is also in keeping with previous calculations.[65,66] As mentioned in Secs. III A and III C, the rearrangement corrections are sizable at negative energies.[5]

We acknowledge useful discussions with J. Lavine and P. J. Siemens.

[1]K. A. Brueckner and J. L. Gammel, Phys. Rev. 109, 1023 (1958).
[2]H. A. Bethe, Annu. Rev. Nucl. Sci. 21, 93 (1971).
[3]K. A. Brueckner, R. J. Eden, and N. C. Francis, Phys. Rev. 100, 891 (1955).
[4]G. L. Shaw, Ann. Phys. (N. Y.) 8, 509 (1959).
[5]N. Azziz, Nucl. Phys. A147, 401 (1970).
[6]A. K. Kerman, H. MacManus, and R. M. Thaler, Ann. Phys. (N. Y.) 8, 551 (1959).
[7]B. Mulligan, Ann. Phys. (N. Y.) 26, 159 (1964).
[8]L. Verlet and J. Gavoret, Nuovo Cimento 10, 505 (1958).
[9]A. S. Reiner, Phys. Rev. 133, B1105 (1964).
[10]Q. Ho-Kim and F. C. Khanna, private communication.
[11]H. R. Kidwai and J. R. Rook, Nucl. Phys. A169, 417 (1971).
[12]T. Hamada and I. D. Johnston, Nucl. Phys. 34, 382 (1962).
[13]D. A. Slanina and H. MacManus, Nucl. Phys. A116, 271 (1968).
[14]L. W. Owen and G. R. Satchler, Phys. Rev. Lett. 25, 1720 (1970).
[15]A. D. MacKellar, J. F. Reading, and A. K. Kerman, Phys. Rev. C 3, 460 (1971).
[16]C. B. Dover and N. Van Giai, Nucl. Phys. A190, 373 (1972).
[17]D. A. Slanina, Ph.D. thesis, Michigan State University, 1969 (unpublished).
[18]N. Van Giai, J. Sawicki, and N. Vinh Mau, Phys. Rev. 141, 913 (1966).
[19]M. Bruneau and N. Vinh Mau, in *Methods and Problems of Theoretical Physics*, edited by J. E. Bowcock (North-Holland, Amsterdam, 1970), p. 333.
[20]N. Vinh Mau, *Theory of Nuclear Structure* (International Atomic Energy Agency, Vienna, 1970), p. 931.
[21]T. F. O'Dwyer, M. Kawai, and G. E. Brown, Phys. Lett. 41B, 259 (1972).
[22]J. Cugnon, Nucl. Phys. A208, 333 (1973).
[23]C. L. Rao, M. Reeves, III, and G. R. Satchler, Nucl. Phys. A207, 482 (1973).
[24]A. Lev, W. P. Beres, and M. Divadeenam, Phys. Rev. Lett. 31, 555 (1973).
[25]A. A. Abrikosov, L. P. Gorkov, and I. E. Dzyaloshinsky, *Methods of Quantum Field Theory in Statistical Mechanics* (Prentice Hall, Englewood Cliffs, New Jersey, 1963).
[26]J. S. Bell and E. J. Squires, Phys. Rev. Lett. 3, 96 (1959).
[27]R. Lipperheide, Z. Phys. 202, 58 (1967).
[28]A. L. Fetter and K. M. Watson, in *Advances in Theoretical Physics*, edited by K. A. Brueckner (Academic, New York, 1965), Vol. 1, p. 115.
[29]J. Hüfner and C. Mahaux, Ann. Phys. (N. Y.) 73, 525 (1972).
[30]R. V. Reid, Ann. Phys. (N. Y.) 50, 411 (1968).
[31]G. E. Brown, *Unified Theory of Nuclear Model and Forces* (North-Holland, Amsterdam, 1971).
[32]S.-O. Bäckman, Nucl. Phys. A130, 427 (1969).
[33]M. Baranger, Comments Nucl. Part. Phys. 4, 81 (1970).
[34]G. E. Brown, Rev. Mod. Phys. 43, 1 (1971).
[35]R. S. Poggioli and A. D. Jackson, Nucl. Phys. A165, 582 (1971).
[36]H. S. Köhler, Nucl. Phys. A204, 65 (1973).
[37]O. Sjöberg, Nucl. Phys. A209, 363 (1973).
[38]O. Sjöberg, Ann. Phys. (N. Y.) 78, 39 (1973).
[39]K. A. Brueckner, Phys. Rev. 103, 172 (1956).
[40]J. R. Rook, private communication.
[41]M. I. Haftel and F. Tabakin, Nucl. Phys. A158, 1 (1970).
[42]S. A. Coon and J. Dabrowski, Phys. Rev. 140, B287 (1965).
[43]P. J. Siemens, private communication.
[44]P. J. Siemens, Nucl. Phys. A141, 225 (1970).
[45]G. E. Brown, J. H. Gunn, and P. Gould, Nucl. Phys. 46, 598 (1963).
[46]G. F. Bertsch and T. T. S. Kuo, Nucl. Phys. A112, 204 (1968).
[47]L. R. B. Elton, Nucl. Phys. 89, 69 (1966).
[48]G. Passatore, Nucl. Phys. A95, 694 (1967).
[49]P. H. Bowen, J. P. Scanlon, G. H. Stafford, J. J. Thresher, and P. E. Hodgson, Nucl. Phys. 22, 640 (1961).
[50]G. L. Thomas and E. J. Burge, Nucl. Phys. A128, 545 (1969).
[51]W. T. H. Van Oers, Phys. Rev. C 3, 1550 (1971).
[52]F. D. Becchetti and G. W. Greenlees, Phys. Rev. 182, 1190 (1969).
[53]F. G. Perey, Phys. Rev. 131, 745 (1963).
[54]G. E. Brown, Comments Nucl. Part. Phys. 4, 75 (1970).
[55]C. A. Engelbrecht and H. Fiedeldey, Ann. Phys. (N. Y.) 42, 262 (1967).
[56]K. Seth, Nucl. Phys. A138, 61 (1969).
[57]F. Perey and B. Buck, Nucl. Phys. 32, 353 (1962).
[58]D. Wilmore and P. E. Hodgson, Nucl. Phys. 55, 673 (1964).
[59]F. Perey, in *Nuclear Structure Study with Neutrons*, edited by M. Nève de Mévergnies, P. Van Assche, and J. Vervier (North-Holland, Amsterdam, 1966), p. 436.
[60]K. A. Brueckner and J. Dabrowski, Phys. Rev. 134, B722 (1964).
[61]G. R. Satchler, *Isospin in Nuclear Physics* (North-Holland, Amsterdam, 1969), p. 389.
[62]G. W. Hoffmann, W. H. Dunlop, G. J. Igo, J. G. Kulleck, J. W. Sunier, and C. A. Whitten, Nucl. Phys. A187, 577 (1972).
[63]J. Dabrowski and A. Sobiczewski, Phys. Lett. 5, 87 (1963).
[64]N. M. Hugenholtz and L. Van Hove, Physica 24, 363 (1958).
[65]K. A. Brueckner and D. T. Goldman, Phys. Rev. 116, 424 (1959).

[66]H. S. Köhler, Phys. Rev. 137, B1145 (1965).
[67]J. Dabrowski and P. Haensel, Phys. Rev. 7, 916 (1972).
[68]P. C. Martin and J. Schwinger, Phys. Rev. 115, 1342 (1959).
[69]G. W. Greenlees, G. J. Pyle, and Y. C. Tang, Phys. Rev. 171, 1115 (1968).
[70]I. R. Afnan and Y. C. Tang, Nucl. Phys. A141, 653 (1970).